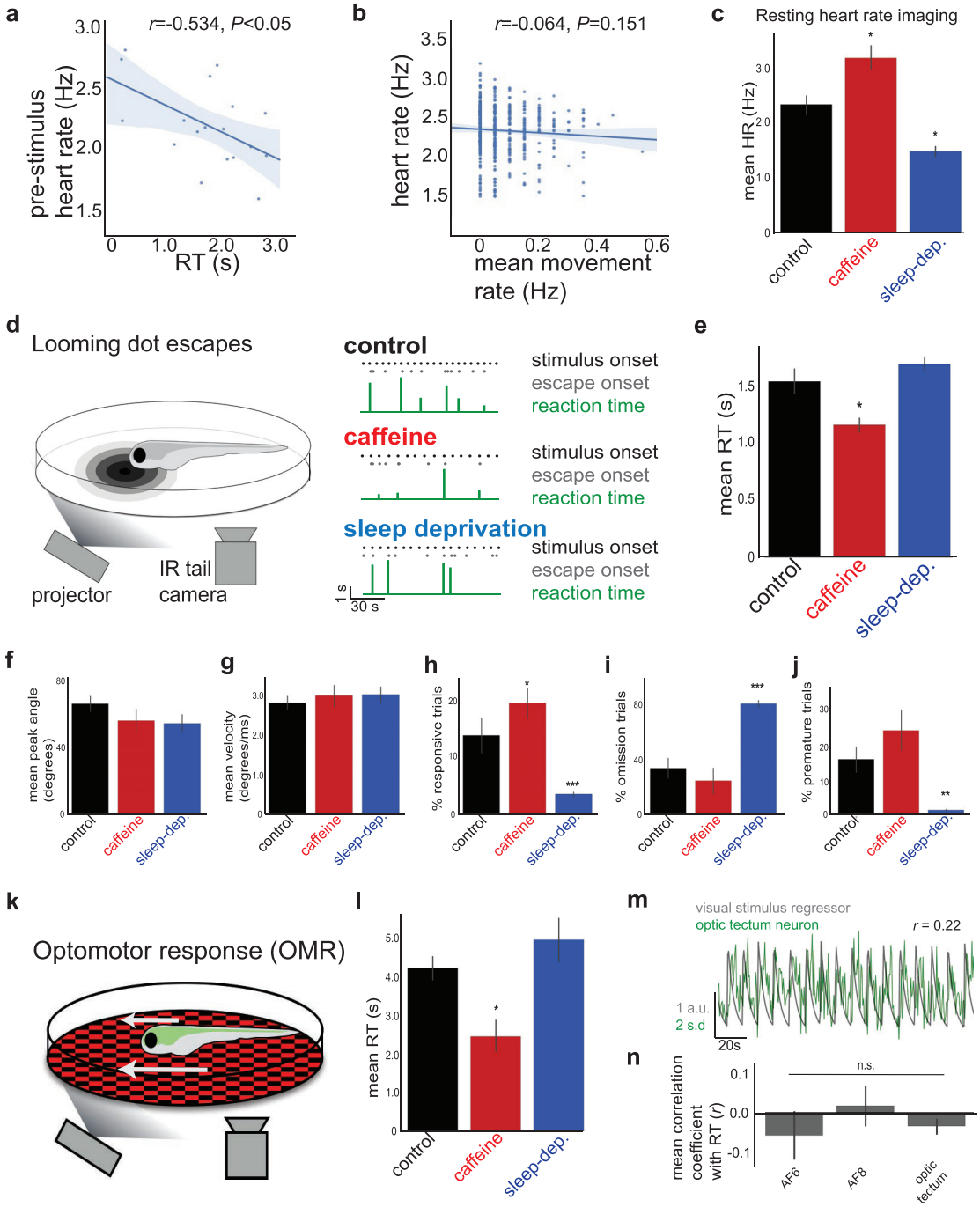

Figure S1. Reaction Time Is a Measure of Internally Generated Alertness States, Related to Figure 1

(A) Correlation between pre-stimulus heart rate and RT in an example fish ($r = -0.534$, $p < 0.05$). Heart rate tends to be higher before fast RTs (high alertness) and tends to be lower before slow RTs (low alertness). See Figure 1E for summary data. Solid line = linear regression; shaded region = 95% confidence interval.

(B) Summary data, showing no significant correlation between heart rate and total movement rate in 20 s bins ($r = -0.064$, $p > 0.05$, n = 6).

(C) Effects of caffeine and sleep deprivation on resting heart rate, imaged in fully embedded fish. n = 6, 4, and 4 (control, caffeine, and sleep-deprivation, respectively). One-way ANOVA, $F_{(2,13)} = 16.41$, $p < 0.001$. Two-sided t tests with control, *$p < 0.05$.

(D) Left: Schematic of zebrafish looming dot RT behavior. Right: Example behavioral recordings over 2 minutes. Each fish is either control (no treatment), treated with 50 mg/L caffeine, or subjected to one night of sleep deprivation. Note that control fish display variability in RTs, whereas fish with potentiated alertness (caffeine) have faster RTs and fish with suppressed alertness (sleep deprivation) have slower RTs.

(E) Summary data for control fish (n = 16, black), fish treated with 50 mg/L caffeine (n = 8, red), and fish deprived of sleep for one night (n = 10, blue). Mean ± SEM. Kruskal-Wallis test, H = 10.67, $p < 0.005$, Mann-Whitney rank tests with control. *$p < 0.05$.

(legend continued on next page)

(F–J) Data from the same fish in panel e. All data are mean ± SEM. (F) Summary data for peak tail angle. Kruskal-Wallis test, $H = 3.75$, $p > 0.05$. (G) Summary data for peak tail velocity. Kruskal-Wallis test, $H = 1.30$, $p > 0.05$. (H) Summary data for % responsive trials. Kruskal-Wallis test, $H = 20.46$, $p < 0.001$. Mann-Whitney rank tests with control. *$p < 0.05$, ***$p < 0.001$. (I) Summary data for % omitted trials. Kruskal-Wallis test, $H = 17.95$, $p < 0.001$. Mann-Whitney rank tests with control, ***$p < 0.001$. (J) Summary data for % premature response trials. Kruskal-Wallis test, $H = 14.88$, $p < 0.001$. Mann-Whitney rank tests with control, **$p < 0.01$. Caffeine does not significantly increase the premature response rate.

(K) Schematic of zebrafish optomotor response (OMR) behavior.

(L) Summary data. Mean ± SEM. Kruskal-Wallis test, $H = 7.56$, $p < 0.05$, Mann-Whitney rank tests with control. *$p < 0.05$.

(M and N) Visual stimulus-correlated neurons in looming-related sensory regions do not show stimulus responses correlated to RT. (M) Example neuron correlated to visual stimulus regressor, recorded with 2-photon imaging (STAR Methods). (N) Summary data for visual-correlated neurons in each looming-associated visual region (AF: retinal arborization field). n = 12, 23, and 217 cells (left to right). Significance values determined by one-sample Wilcoxon signed-rank tests and false discovery rate correction for multiple comparisons. Mean ± SEM. All summary data are grouped by fish.

a **Commands for registration in CMTK**

all volumes saved in mm scale, as .nrrd
all transform files saved as .xform

Rigid step (Affine)
cmtk make_initial_affine --centers-of-mass <path to live GCaMP volume> <path to fixed GCaMP volume> <path to save initial affine transform>

cmtk registration -v --mi --initial <path to initial affine transform> --auto-multi-levels 4 --histogram-equalization-flt --histogram-equalization-ref --match-histograms --dofs 6,12 -o <path to save affine transform> <path to live GCaMP volume> <path to fixed GCaMP volume>

Non-rigid warping step (B-splines)
cmtk warp -v -o <path to save warp transform> --grid-spacing 0.1 --refine 6 --jacobian-weight 0.05 --rigidity-weight 0.1 --exploration 0.01 --accuracy 0.0001 --match-histograms --exact-spacing --mi --output-intermediate --initial <path to affine transform> <path to live GCaMP volume> <path to fixed GCaMP volume>

Apply transformation to each fixed channel
cmtk reformatx -v -o <path to save warped GCaMP volume> --floating <path to fixed GCaMP volume> <path to live GCaMP volume> <path to warp transform>

cmtk reformatx -v -o <path to save warped antibody1 volume> --floating <path to fixed antibody1 volume> <path to live GCaMP volume> <path to warp transform>

cmtk reformatx -v -o <path to save warped antibody2 volume> --floating <path to fixed antibody2 volume> <path to live GCaMP volume> <path to warp transform>

cmtk reformatx -v -o <path to save warped antibody3 volume> --floating <path to fixed antibody3 volume> <path to live GCaMP volume> <path to warp transform>

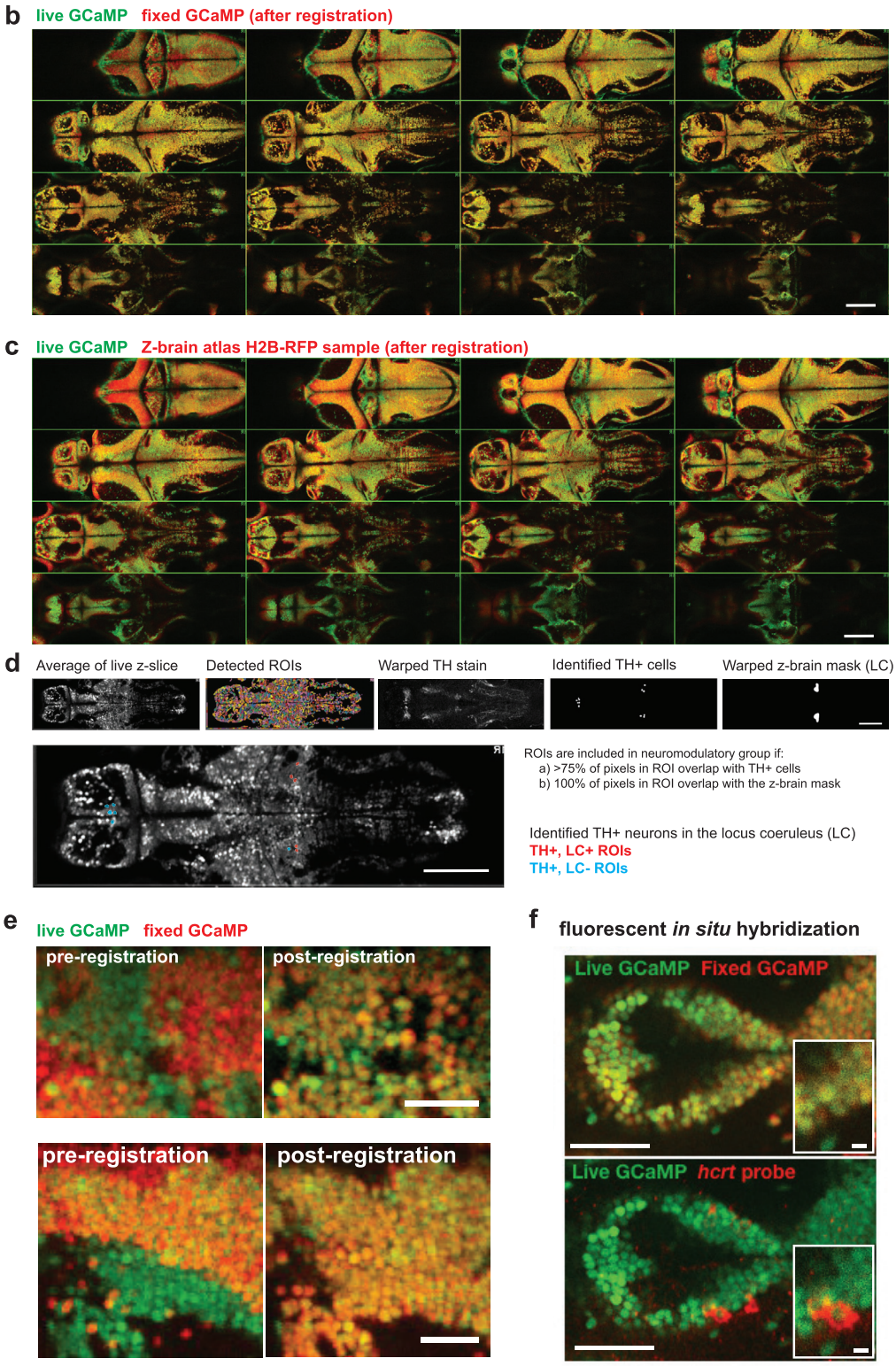

Figure S2. Additional Details of MultiMAP and Compatibility with *In Situ* Hybridization, Related to Figure 2

(A) For general user reference: commands used for volume registration in CMTK (STAR Methods).

(B) 16 z-planes extracted from tissue volumes, from a single example fish. Live GCaMP (green) and fixed GCaMP after registration (red); yellow indicates overlap. Each plane corresponds to z-plane in live volume that was imaged during behavior.

(legend continued on next page)

(C) 16 z-planes extracted from tissue volumes, in same example fish as panel b. Live GCaMP (green) and Z-brain atlas *Tg(elavl3:H2B-RFP)* reference after registration (red).

(D) Protocol for annotation of live-recorded cells with neurochemical and anatomical information, with example for TH+ cells in the locus coeruleus (LC). To distinguish between antibody labeling of cell bodies versus axonal and dendritic projections, cell bodies were manually identified. For each ROI identified from live-imaged z-plane, the ROI is assigned to a given neuromodulatory region if 75% of the pixels within that ROI overlap with the antibody cell body label, and 100% of the pixels within that ROI overlap with the anatomical region label(s). In the example image, TH+ LC neurons are labeled in red, whereas TH+ cells that do not overlap with the LC anatomical mask are labeled in blue. Scale bars: 100 μm.

(E) Higher magnification images of example brains, showing cellular-resolution of registration approach, even in densely packed tissue. Scale bars: 30 μm.

(F) Demonstration of registration method compatibility with fluorescent *in situ* hybridization (fISH). Here we show registration in the hypothalamus, even after the harsh treatment of fISH. We used the hybridization chain reaction method (STAR Methods), which allows for multiplexed molecular labeling with orthogonal fluorophores. Detection of RNA over protein is particularly useful for neuropeptides such as hypocretin/orexin (*hcrt*, used here), where the protein is primarily localized to axonal terminals. Scale bars: 50 μm and 5 μm (inset).

Neuromodulatory group/ number of fish and cells	Z-brain masks	Antibody stain	RT-neural activity scatterplot	r-value distribution
hypocretin/orexin (n=12; 69)	[1]	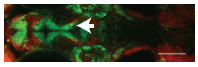		
CART (n=3; 13)	[1]	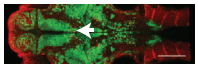		
Galanin (n=5; 28)	[1]	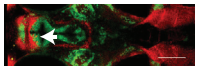		
NPVF (n=5; 33)	[1]	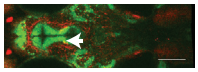		
NPY (n=5; 25)	[1]	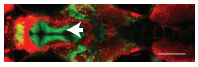		
SOM (n=6; 44)	[1]	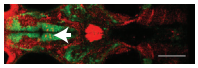		
5HT-pineal (n=3; 63)	[55]			
5HT-hypothalamus (n=4; 349)	[16,35,74]	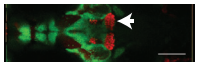		
5HT-superior raphe (n=4; 90)	[218]	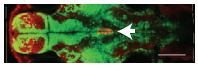		
5HT-inferior raphe (n=4; 17)	[217]	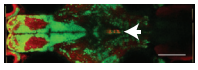		
5HT-pretectum (n=4; 32)	[13,66,76]	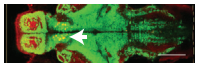		
5HT-hindbrain (n=4,28)	[225]	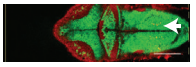		
NE-medulla oblongata (n=8,67)	[125,200]	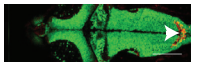		
NE-locus coeruleus (n=14,84)	[219,220]	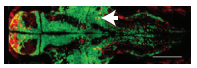		
DA-pretectum (n=15,169)	[13,66,76]			
DA-posterior tuberculum (n=15; 123)	[7,8]			
DA-hypothalamus (n=16; 296)	[9,10,11,12,35,74]			
DA-telencephalon (n=16; 138)	[283,291]			
ChAT-tectum (n=10; 67)	[106]			
ChAT-tegmentum (n=13; 280)	[97,98,108]			
ChAT-dorsal hindbrain (n=9; 60)	[225]			
ChAT-ventral hindbrain (n=12; 253)	[222,223,224]			

(legend on next page)

Figure S3. Anatomical and Functional Details of the 22 Neuromodulatory Cell Types Imaged in Zebrafish, Related to Figures 3 and 4

From left: name of neuromodulatory group and number of fish and cells analyzed, list of Z-brain masks to identify anatomical location of cells (out of 294), overlay of GCaMP6s and antibody in example z-plane (neurons location denoted with white arrow), RT-neural activity scatterplot from an example neuron, and the distribution of correlation coefficients for all neurons recorded.

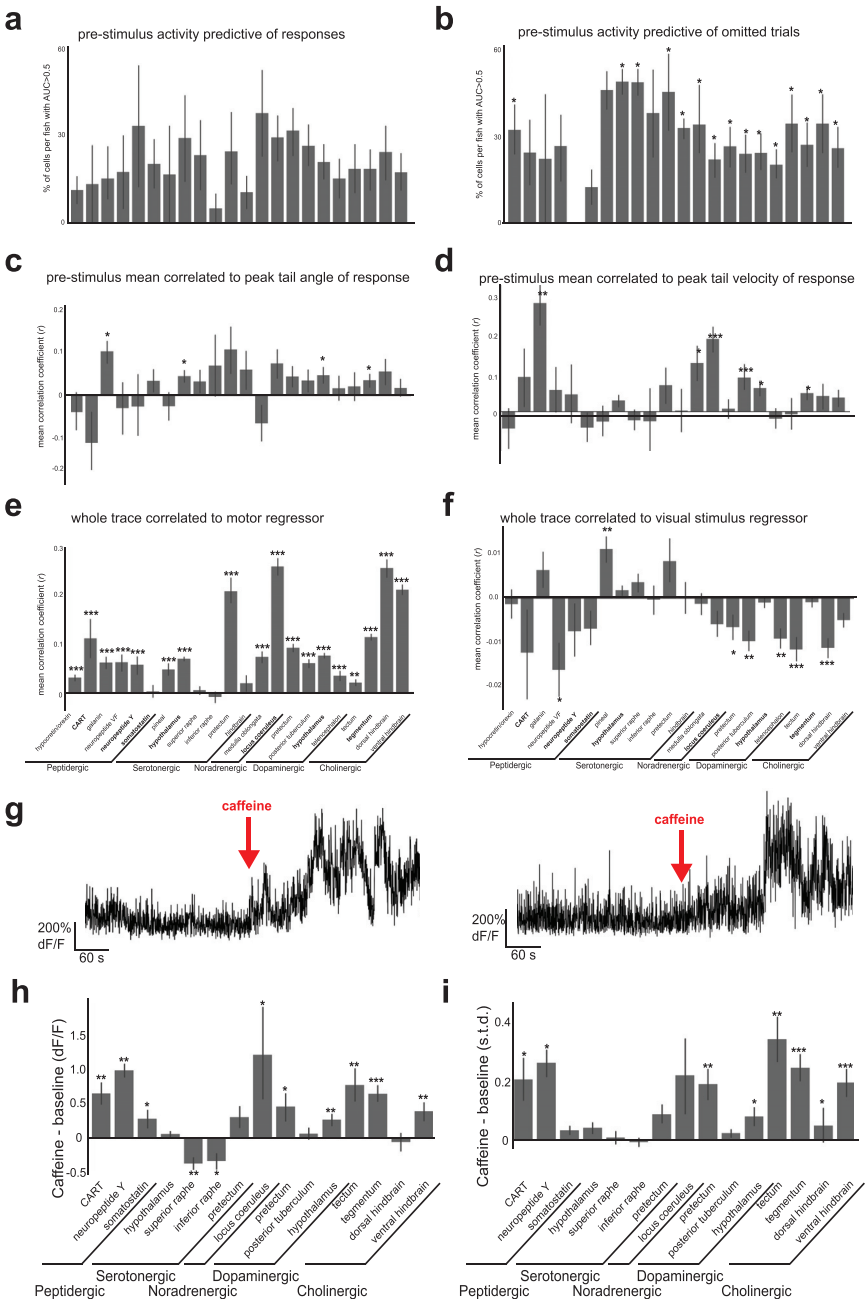

Figure S4. Additional Functional Characterization of Neuromodulatory Cell Types in Zebrafish, Related to Figures 3 and 4

(A–F) Data derived from the same fish used in Figure 3C. Significance values determined by one-sample Wilcoxon signed-rank tests and false discovery rate correction for multiple comparisons. *$p < 0.05$, **$p < 0.01$, ***$p < 0.001$. (A) Percentage of neurons per fish that distinguish response trials from all other trials, using logistic regression (area under ROC curve > 0.5). (B) Percentage of neurons per fish that distinguish omitted trials from all other trials, using logistic regression (area under ROC curve > 0.5). (C) Correlation between pre-stimulus activity and post-stimulus peak tail angle. (D) Correlation between pre-stimulus activity and post-stimulus peak tail velocity. (E) Correlation between each neuron's entire trace and a regressor of classified tail turns. (F) Correlation between each neuron's entire trace and a regressor of visual stimulus onset.

(G) Example traces from two cholinergic neurons in the tegmentum.

(H and I) Summary data, showing difference between pre- and post- caffeine mean (H) and standard deviation (I). n = 3 fish for each cell type (n = 15,9,6,13,16,12,7,8,11,27,32,16,45,33,24 cells, from left to right). Significance values determined by one-sample Wilcoxon signed-rank tests and false discovery rate correction for multiple comparisons. Mean ± SEM. *$p < 0.05$, **$p < 0.01$, ***$p < 0.001$.

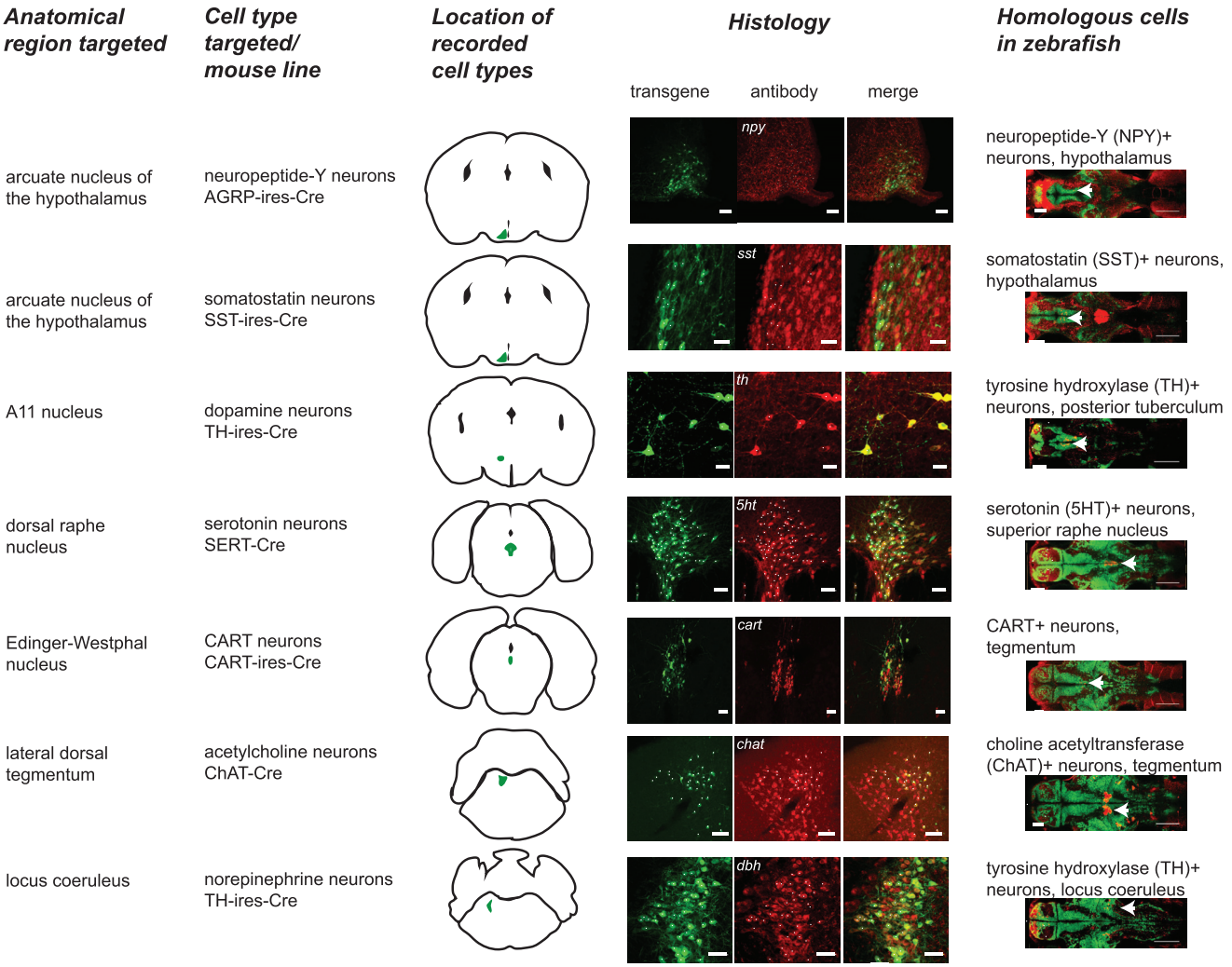

Figure S5. Anatomical and Targeting Details of the Seven Neuromodulatory Groups Tested in Mice, Related to Figures 5 and 6

From left: name of anatomical region targeted, name of cell type targeted and Cre line used, schematic of recording location (GCaMP-expressing region shaded in green), co-labeling of antibody label with GCaMP, ChR2-eYFP, or eNpHR3.0-eYFP expression (matching cells denoted by white dots), and homologous neuromodulatory group in larval zebrafish (from Figure S3 and STAR Methods). Scale bars: 50 μm (arcuate nucleus - npy), 20 μm (arcuate nucleus - sst), 20 μm (A11), 50 μm (dorsal raphe), 50 μm (Edinger-Westphal nucleus), 50 μm (locus coeruleus), 100 μm (lateral dorsal tegmentum), 100 μm (zebrafish images).

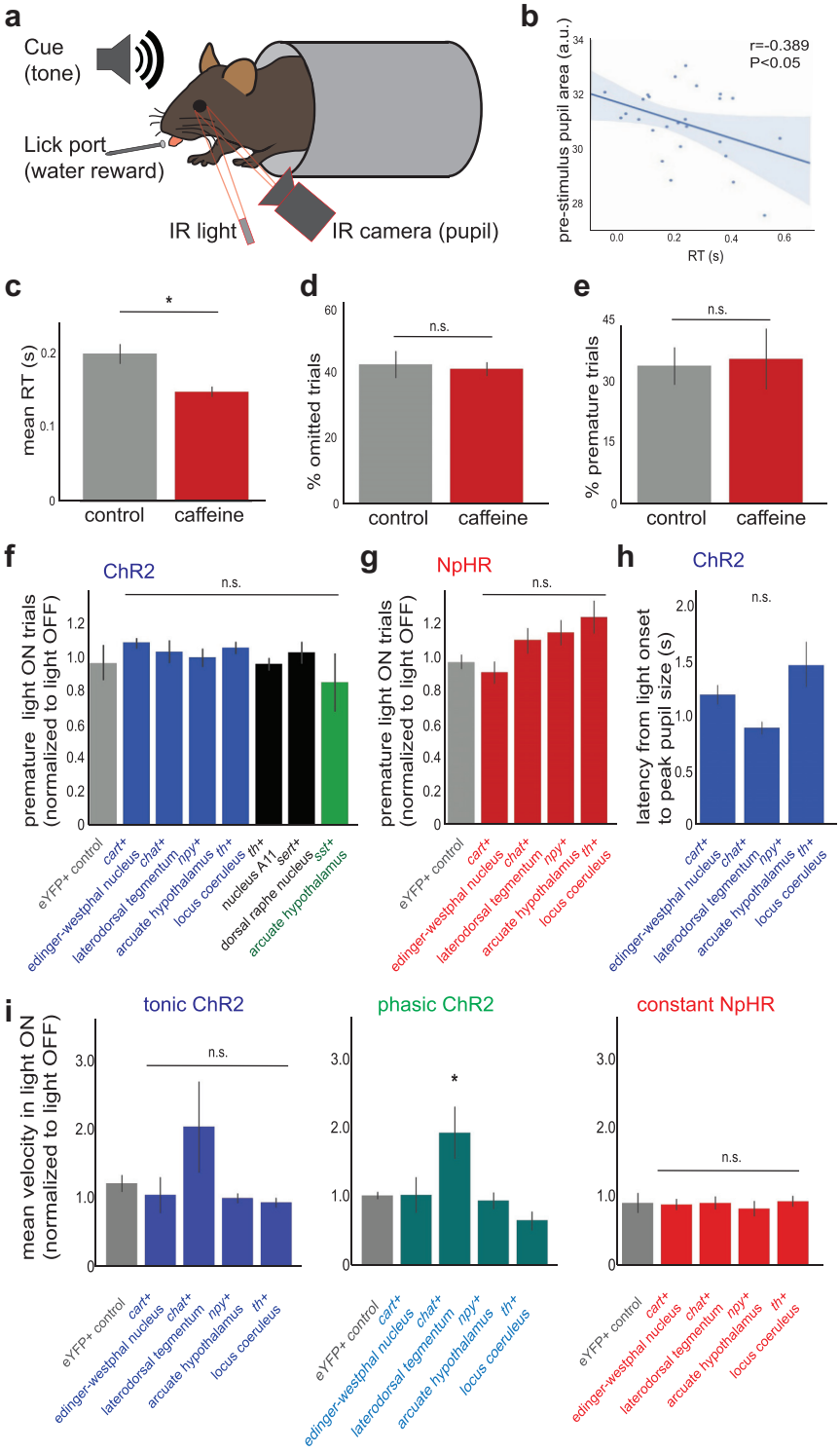

Figure S6. Behavioral Controls for Mouse Behavior, Related to Figures 5 and 6

(A) Schematic of mouse behavioral task with simultaneous measurement of pupil area. Head-fixed mice report the presence of a 500 ms auditory stimulus by contacting a lick port, which results in a water reward if contacted within 1 s of stimulus onset. Pupil size is recorded by an infrared (IR) camera. Larger pupil size reflects higher alertness state.

(B) Scatterplot of mean pre-stimulus pupil area (arbitrary units, a.u.) and RT in an example mouse. The pupil tends to be larger before fast RTs (high alertness) and tends to be smaller before slow RTs (low alertness). Solid line = linear regression, shaded region = 95% confidence interval. $R = -0.389$, $p < 0.05$.

(legend continued on next page)

(C–E) Data for mice injected with saline (n = 3, black), or 20 mg/Kg caffeine (n = 3, red). (C) Summary data for RT. Mean ± SEM, Student's t test. *p < 0.05. (D) Summary data for percent omitted trials. Mean ± SEM, Student's t test, p = 0.81. (E) Summary data for percent premature trials. Mean ± SEM, Student's t test, p = 0.87.

(F and G) Data for same mice used in Figures 6B and 6C, showing premature trials (% premature light ON trials, normalized by % premature light OFF trials). (F) Summary data for optogenetic activation. Bars are mean ± SEM, n = 27 mice (n = 5,3,3,4,3,3,3,3, from left to right). Significance values were determined by permutation tests with the eYFP control group, and false discovery rate correction for multiple comparisons. (G) Summary data for optogenetic inactivation. Bars are mean ± SEM, n = 18 mice (n = 4,3,4,3,4, from left to right). Significance values were determined by permutation tests with the eYFP control group, and false discovery rate correction for multiple comparisons.

(H) Latency from light onset to the peak of the pupil signal, for the three cell types with significant increases pupil upon optogenetic activation (from Figure 6E). One-way ANOVA, $F_{(2,9)} = 4.35$, $p > 0.05$).

(I) Mice were placed in an open field and their behavior was quantified before and during optogenetic activation (tonic or phasic) or inactivation of the four cell types with significant correlations to RT (from Figure 5D). Mean velocity during the 5 minute light ON period, normalized to the preceding 5 m light OFF period, for tonic ChR2 (473 nm light at 5 Hz; left), phasic ChR2 (473 nm light at 20 Hz for 500 ms every 2 s; middle), or constant NpHR (589 nm light continuously). n = 20 mice for ChR2 experiments (n = 4,4,4,4,4, from left to right), n = 20 mice for NpHR experiments (n = 5,3,4,4,4, from left to right). Significance values were determined by permutation tests with the eYFP control group, and false discovery rate correction for multiple comparisons. *p < 0.05.